Available online at www.sciencedirect.com
ScienceDirect
Journal of Power Sources 171 (2007) 448–456
JOURNAL OF POWER SOURCES
www.elsevier.com/locate/jpowsour

Screening of electrocatalysts for direct ammonia fuel cell: Ammonia oxidation on PtMe (Me: Ir, Rh, Pd, Ru) and preferentially oriented Pt(1 0 0) nanoparticles

F.J. Vidal-Iglesias, J. Solla-Gullón *, V. Montiel, J.M. Feliu, A. Aldaz

Instituto de Electroquímica, Universidad de Alicante, Apartado 99, 03080 Alicante, Spain

Received 29 March 2007; received in revised form 28 May 2007; accepted 9 June 2007
Available online 17 June 2007

Abstract

Ammonia has attracted attention as a possible fuel for direct fuel cells since it is easy to handle and to transport as liquid or as concentrated aqueous solution. However, on noble metal electrodes ammonia oxidation is a sluggish reaction and the electrocatalyst needs to be improved for developing efficient ammonia fuel cells. In this work, ammonia electrooxidation reaction on 3–4-nm bimetallic PtMe (Ir, Rh, Pd, Ru) and on preferentially oriented Pt(1 0 0) nanoparticles is reported. PtMe nanoparticles have been prepared by using water-in-oil microemulsions to obtain a narrow size distribution whereas preferentially oriented Pt nanoparticles have been prepared through colloidal routes. Among all the bimetallic samples tested, only $Pt_{75}Ir_{25}$ and $Pt_{75}Rh_{25}$ nanoparticles show, at the low potential range, an enhancement of the oxidation density current with respect to the behaviour found for pure platinum nanoparticles prepared by the same method. In addition, two Pt(1 0 0) preferentially oriented nanoparticles of different particle size (4 and 9 nm) have been also studied. These oriented nanoparticles show higher current densities than polycrystalline Pt nanoparticles due to the sensitivity of ammonia oxidation toward the presence of surface sites with square symmetry. The reactivity of the different 4-nm nanoparticles parallels well with that expected from bulk PtMe alloys and Pt single crystal electrodes.

Keywords: Bimetallic PtMe nanoparticles; Preferentially oriented Pt(1 0 0) nanoparticles; Ammonia electrooxidation; Alloys; Electrocatalysis

1. Introduction

The study of the electrochemical behaviour of ammonia is an important topic in the field of environmental electrochemistry, not only from the point of view of its electrochemical elimination from wastewater streams, but also for water and air analysis by employing electrochemical sensors [1–4]. In addition, ammonia has attracted attention as a possible fuel for direct fuel cells [5] since it is easy to handle and to transport as liquid or as concentrated aqueous solution. Its equilibrium potential is low:

$$N_2 + 6H^+ + 6e^- \Leftrightarrow 2NH_3(aq), \qquad E^\circ = -0.092\,V$$

and the theoretical charge for oxidation to N_2 is 4.75 Ah g^{-1} that compares very well with the theoretical charge of methanol in its oxidation to CO_2 5.02 Ah g^{-1}. However, the direct oxidation of ammonia is a sluggish reaction on noble metals and new electrocatalysts should be found to improve the behaviour of a direct ammonia fuel cell. In spite of the fact that this reaction has been scrutinized for through many years, very few papers have been focused on the search of new electrocatalysts. Recently, we have shown that ammonia oxidation on platinum is an extremely surface sensitive reaction [6,7] which takes place almost exclusively on surface sites with (1 0 0) symmetry. In addition, Rosca and Koper [8] also studied the electrocatalytic oxidation of ammonia on Pt(1 1 1) and Pt(1 0 0) not only using voltammetry and chronoamperometry but also *in situ* infrared spectroscopy measurements. As a consequence, the use of (1 0 0) preferentially oriented platinum nanoparticles is a practical strategy to increase the electrocatalytic activity of platinum electrodes.

The most widely accepted mechanism for ammonia oxidation was proposed by Gerischer and Mauerer in 1970 [9]. The authors proposed that the ammonia molecule, after being adsorbed, is dehydrogenated to different adsorbed intermediate species (NH_x, where $0 \le x \le 2$). Nitrogen is formed by reaction of these species react with OH^-. Whereas, NH_{ad} and $NH_{2,ad}$ are considered as active intermediates for N_2 formation, N_{ad},

* Corresponding author. Tel.: +34 965903535; fax: +34 965903537.
E-mail address: jose.solla@ua.es (J. Solla-Gullón).

0378-7753/$ – see front matter © 2007 Elsevier B.V. All rights reserved.
doi:10.1016/j.jpowsour.2007.06.015

formed by further dehydrogenation, remains strongly adsorbed on the surface acting as a poison.

De Vooys et al. have studied the activity for ammonia oxidation and the intermediates formed during the oxidation on polycrystalline surfaces of platinum, palladium, rhodium, ruthenium, iridium, copper, silver and gold [10]. They concluded that only platinum and iridium combine a good capability to dehydrogenate ammonia with a sufficiently low affinity to produce adsorbed nitrogen atoms (N_{ad}). Thus, the authors also concluded that platinum is the best catalyst for this reaction, due to the fact that N_{ad} is formed at very high potentials in comparison with other metals. Moreover, Endo et al. [11,12] have studied the electrochemical behaviour of some PtMe alloy surfaces (PtIr, PtCu, PtRu and PtNi) reporting that only the presence of Ru and Ir could improve the catalytic properties of platinum.

To our knowledge, no others papers have been yet published in relation to the search and testing of new dispersed electrocatalysts for ammonia oxidation. In addition, it is important to remark that all previous studies were performed with bulk alloys of different atomic compositions but not with dispersed nanoparticles, which are considered as required material for practical purposes. This study has been carried out following two different approaches. On the one hand, and due to the high sensitivity of this reaction toward Pt(1 0 0) sites, a sample containing cubic platinum nanoparticles with a lower particle size (4 nm) than those employed in our previous studies (9 nm) [13,14] has been prepared, characterised and tested as suitable electrocatalyst. It is important to remind that oxidation current densities about seven times higher than that obtained for non-oriented nanoparticles were reported with preferentially oriented Pt(1 0 0) nanoparticles of ≈9 nm [13,15]. On the other hand, it is well known that the use of platinum-based binary catalyst is an attractive alternative to improve the electrocatalytic performance of some oxidation reactions [16]. Thus, different PtMe nanoparticles have been prepared and studied. In these binary nanoparticles, Pt is employed as base metal not only because of its electrocatalytic properties but also due to the fact that N_{ad} is formed at very high potentials on its surface in comparison with other metals.

In addition, it is important to state whether 4-nm nanoparticles exhibit properties different to those reported for bulk materials. This would clarify whether the reactivity is related to intrinsic properties associated with the size of the electrocatalytic materials or to other effects, e.g. related to the substrate or the surface composition. Therefore, in this work, some recent results about the synthesis, characterisation and electrochemical behaviour of PtMe nanoparticles (Me = Ir, Pd, Rh and Ru) as well as small (≈4 nm) cubic platinum nanoparticles are reported.

2. Experimental

2.1. Preparation and physico-chemical characterisation of the nanoparticles

Pt, Me and PtMe nanoparticles were synthesized by reduction of H_2PtCl_6, $RuCl_3$, K_2PdCl_4, $IrCl_4$ or $Rh(NO_3)_3$, with sodium borohydride using a water-in-oil microemulsion of water/polyethyleneglycol-dodecylether (BRIJ®30)/*n*-heptane in a similar way to that previously reported [17–23]. Among the advantages of this technique it is important to highlight not only the simplicity to prepare the nanoparticles with uniform size and composition but also the capability of cleaning the surface of the nanoparticles avoiding change the surface structure and composition of the nanoparticles [21,22,24].

Preferentially oriented Pt(1 0 0) nanoparticles were prepared using two different colloidal routes. Large (≈9 nm) Pt nanoparticles were synthesised using the same methodology to that previously reported [13–15]. Very briefly 0.1 ml of a 0.1 M sodium polyacrylate solution was added to a 100 ml of an aged 1×10^{-4} M K_2PtCl_4 solution. After 20 min of Ar bubbling, the Pt ions were reduced by bubbling H_2 for 5 min. The reaction vessel was then sealed and the solution was left overnight. After complete reduction (12–14 h) two NaOH pellets were added to produce the precipitation of the nanoparticles. After complete precipitation, the nanoparticles were washed 3–4 times with ultra-pure water. Finally, small Pt(1 0 0) nanoparticles (≈4–5 nm) were synthesized according to the procedure described in Ref. [25]. Briefly, 20 mL of a 1×10^{-2} M $NaBH_4$ solution aged for 3 h was added dropwise to 20 mL of a 6.5×10^{-4} M K_2PtCl_6 solution with vigorous stirring at ice-cold temperature. After complete reduction, the nanoparticles were washed 3–4 times with ultra-pure water.

X-ray photoelectron spectroscopy (XPS) measurements were performed with a VG-Microtech Multilab, using a Mg Kα (1253.6 eV) source. Transmission electron microscopy (TEM) experiments were performed with a JEOL, JEM-2010 microscope working at 200 kV. The images were analysed with the analySIS 3.0 program. For each sample, usually over more than 300 particles from different parts of the grid were used to estimate the mean diameter and size distribution of the nanoparticles. Energy dispersive analysis by X-rays (EDAX) was obtained with an OXFORD, INCA model system.

2.2. Preparation of the electrodes and electrochemical measurements

The procedure used for the electrochemical study has been previously reported [21,26–28]. Briefly, as current collector a polycrystalline gold disc electrode (5 mm diameter) was used, on which nanoparticles were deposited. Metal nanoparticles were transferred to the gold collector by depositing a drop (generally 5–10 μL) of the nanoparticle suspension in water on the surface of the gold disc; this deposition would represent a maximum amount of ≈6 μg in the case of Pt. A three-electrode electrochemical cell was used. The electrode potential was controlled using a PGSTAT30 AUTOLAB system. The counter electrode was a large area gold wire spiral. Potentials were measured against a reversible hydrogen electrode (RHE) connected to the cell through a Luggin capillary. Potentials are quoted versus this reference electrode. Before each experiment, the gold collector was mechanically polished with alumina and rinsed with ultra-pure water to eliminate the nanoparticles from previous experiments. All the electrochemical measurements were performed in a 0.5 M H_2SO_4 solution at room temperature.

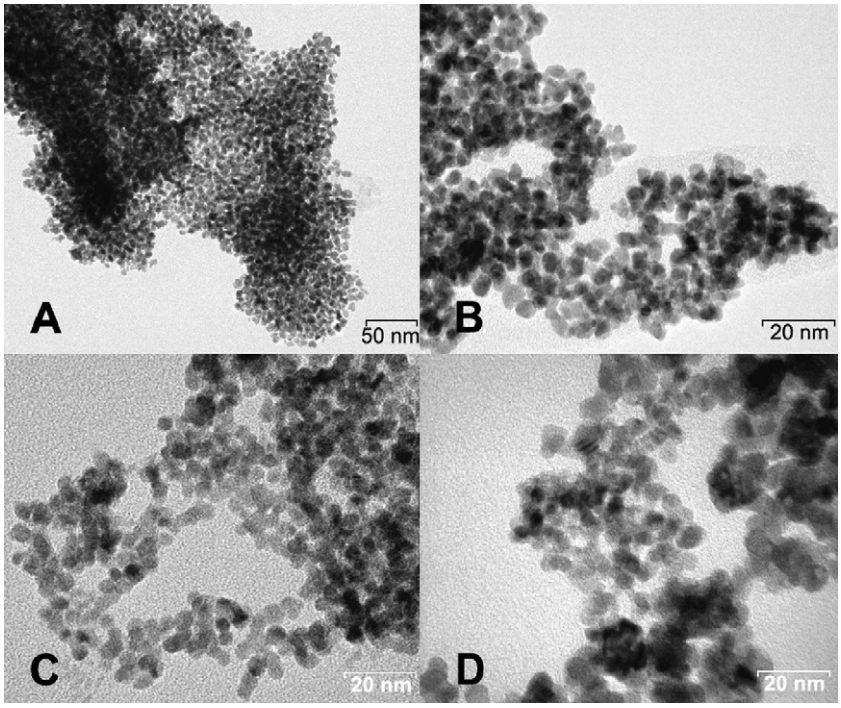

Fig. 1. Representative TEM images for Pt (A), $Pt_{50}Ir_{50}$ (B), $Pt_{25}Rh_{75}$ (C) and $Pt_{20}Pd_{80}$ (D) nanoparticles prepared in microemulsion and dispersed in ultrapure water.

Electrolyte solutions were prepared from Milli-Q® water and Merck p.a. sulphuric acid every day an experiment was carried out. The ammonia solution (0.1 M) was obtained by addition of $(NH_4)_2SO_4$ to a 0.2 M NaOH solution. Both reagents were of p.a. quality (Merck). Solutions were de-oxygenated by bubbling Ar during 20 min.

Following the procedure previously described [21,22,26–28], prior to the use of the nanoparticles for ammonia oxidation, they were cleaned by CO adsorption and stripping, after which the base voltammograms were recorded in 0.5 M H_2SO_4 not only to calculate the real surface area of the catalyst but also to assess the surface cleanliness.

The real catalyst surface area was measured from the charge involved in the so-called hydrogen adsorption–desorption region. For the pure metal nanoparticles, Pt, Ir, Pd and Rh, the values of 210, 218, 212 and 221 $\mu C\,cm^{-2}$ were used respectively [29]. For the PtMe nanoparticles the weighted arithmetic mean between the two pure metals was used. In the case of Ru and PtRu alloys, CO monolayer oxidation charge was used in order to calculate the surface area. This process is a two-electron oxidation reaction. Behm et al. measured that the maximum coverage for Pt is 0.75 [30] being very close to the saturation coverage of 0.8 monolayers estimated for an average of the low index faces [31]. In the calculation of the surface area for Ru nanoparticles, we assumed that the CO_{ad} saturation coverages are similar for both Pt and Ru as it has been previously assumed by Behm et al. [32]. Therefore, 0.75 monolayers was the value used as the CO_{ad} saturation coverage for Ru. In addition, Behm et al. [33] also reported that gas phase CO adsorption experiments on PtRu surface alloys indicate that there is a slight variation in the CO saturation coverage, with slightly lower CO coverages at about equal Pt and Ru surface concentrations. But this effect was reported to be small (lower than 10%), so we will not include it here for the calculation.

3. Results

3.1. Physico-chemical characterisation

Fig. 1 shows some representative TEM images of the nanoparticles prepared in microemulsion and dispersed in water after the chemical decontamination [21,22,24]. From TEM results, it is possible to estimate the particle size that was very similar in all cases and ranging around 3–4 nm, see Table 1. EDX and XPS measurements revealed that the bulk atomic composition is very close to the nominal composition as expected from the synthesis, Table 1 (in the case of PtIr, EDX was not employed to determine the atomic composition of the sample due to the overlapping of the Pt and Ir signals). Moreover, XPS data showed that the nanoparticles are mainly in its metallic state.

3.2. Electrochemical results

Fig. 2 shows the base voltammograms corresponding to the pure metal nanoparticles employed in this study in 0.5 M H_2SO_4. All voltammograms show voltammetric profiles very similar to those obtained for the corresponding metals in bulk state [29]. No evidences are found in relation to the presence of preferential surface orientation and therefore, the surface of the nanoparticles can be considered as polyoriented or polycrystalline. In addition, these base voltammograms clearly evidence the cleanliness of the surface of the nanoparticles: in the case of Pt nanoparticles the sharpness and the symmetry of the peaks which involve

Table 1
Size measured by TEM and composition measured by XPS and EDX of the different nanoparticles used in this work

Nanoparticle	Size (nm)	Atomic composition (XPS)	Atomic composition (EDX)
4-nm Pt_{poly}	4.0 ± 0.6		
9-nm $Pt_{nano-100}$	9.0 ± 3.0		
4-nm $Pt_{nano-100}$	4.4 ± 0.8		
$Pt_{75}Ir_{25}$	4.4 ± 0.9	80.1/19.9	
$Pt_{50}Ir_{50}$	4.0 ± 1.0	51.0/49.0	
$Pt_{25}Ir_{75}$	3.5 ± 0.9	21.9/78.1	
Ir	2.7 ± 0.6		
$Pt_{75}Rh_{25}$	3.8 ± 0.9	80.1/19.9	75.0/25.0
Rh	4.0 ± 1.0		
$Pt_{80}Pd_{20}$	3.5 ± 0.6	75.3/24.7	79.2/20.8
Pd	2.4 ± 0.2		
$Pt_{80}Ru_{20}$	3.4 ± 0.5	76.7/23.3	78.8/21.2
$Pt_{50}Ru_{50}$	3.6 ± 0.6	45.8/54.2	46.4/53.6
$Pt_{20}Ru_{80}$	3.8 ± 0.7	18.9/81.1	19.8/80.2
Ru	4.2 ± 0.7		

fast adsorption–desorption processes (H and anion) prove this statement at first sight.

Fig. 3 shows the results for ammonia oxidation reaction in basic media on the pure metal nanoparticles dispersed on the gold surface. De Vooys et al. concluded that Pt and Ir are the most interesting catalysts for ammonia oxidation in alkaline media [10]. In the same paper, they also reported that Rh, Pd and Ru dehydrogenate the ammonia molecule at significantly lower potentials than on platinum and iridium, leading to the surface poison N_{ads} at much lower potentials than on platinum and iridium. This fact would explain why ruthenium, rhodium and palladium are not active in the oxidation of ammonia to N_2. In agreement with these previous results, in Fig. 3 and for platinum and iridium nanoparticles, well marked oxidation peaks

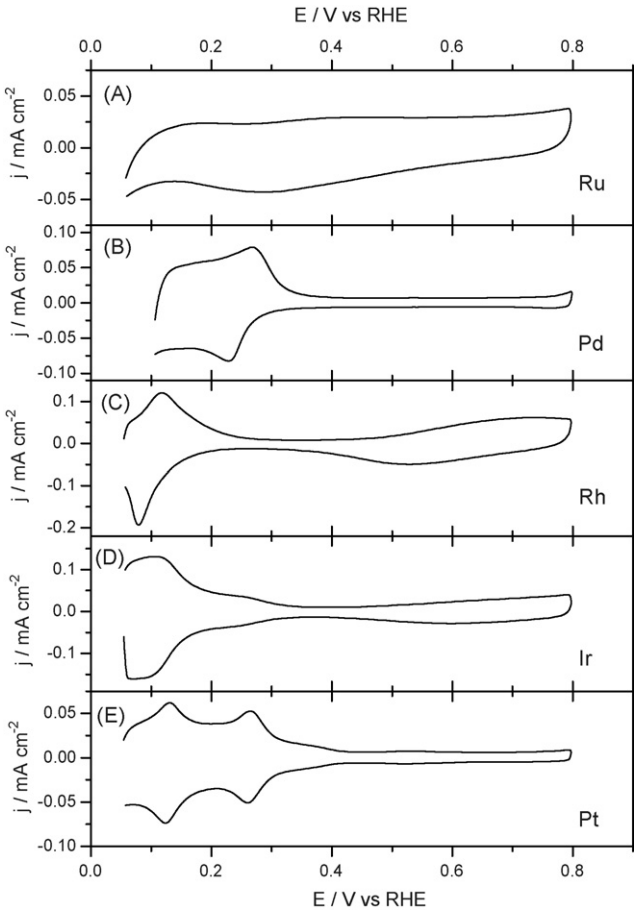

Fig. 2. Voltammetric profiles in H_2SO_4 0.5 M for Ru, Pd, Rh, Ir and Pt nanoparticles prepared in microemulsion. Sweep rate: 50 mV s^{-1}.

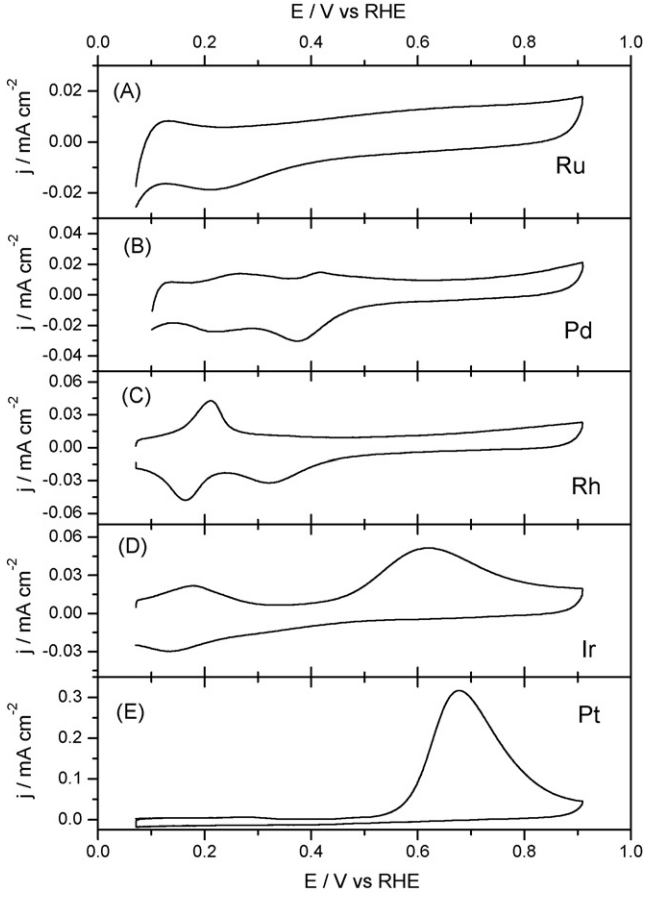

Fig. 3. Ammonia oxidation Ru, Pd, Rh, Ir and Pt nanoparticles prepared in microemulsion. Test solution: NaOH 0.2 M + NH_3 0.1 M. Sweep rate: 10 mV s^{-1}.

at 0.68 and 0.62 V can be respectively observed. For iridium nanoparticles, in spite of the fact that the oxidation current density is not as high as on platinum, the oxidation starts at much lower potentials than on platinum, which may be explained by the fact that Ir needs less positive potentials to dehydrogenate ammonia. As it was previously reported for the bulk metals, in the case of rhodium, palladium and ruthenium, ammonia oxidation practically does not take place within this potential range due to the fast formation of N_{ads}, which blocks the surface.

Once ammonia oxidation on pure metal nanoparticles was analysed, some different PtMe nanoparticles were tested. As it was previously mentioned, all binary nanoparticles were initially characterised in sulphuric acid solution in order to confirm their cleanliness and also to calculate their surface area from the charge density in the so-called hydrogen adsorption–desorption region. From the results obtained with the pure metal nanoparticles, PtIr nanoparticles were initially considered as a promising candidate for ammonia oxidation. Fig. 4 presents the results for the ammonia oxidation for some PtIr nanoparticles of different atomic compositions. Unfortunately, the addition of Ir originates a severe decrease on the ammonia oxidation peak current. For instance, the main oxidation peak diminishes from 0.326 to 0.197 mA cm^{-2} only after changing the atomic composition from pure Pt to $Pt_{75}Ir_{25}$ nanoparticles. That means that only with a 25% Pt decrease, the current density of the main oxidation peak falls about a 40%. This fact indicates that the combination of Ir and Pt does not improve the behaviour of pure Pt towards ammonia oxidation. The results suggest that the distribution of Pt and Ir on the surface of the nanoparticles could be inhomogeneous, i.e. separate Pt regions and Ir regions could coexist on the surface. Nevertheless, it is known that one of the major problems when nanoparticles are employed is to know the "real" atomic surface composition of the nanoparticles. The solution for this problem is not trivial, especially because, until we know, only LEIS (low-energy ion scattering) measurements are able to determine the atomic composition of the outer atomic layer [34]. Therefore, it is necessary to point out that although XPS is considered as a surface probe, the signals are coming from a ≈1 nm layer. Thus, in the case of 4 nm nanoparticles, this depth cannot be considered to be mainly related to the surface compositions as it could be assumed for bulk alloys. An interesting alternative solution to evaluate both surface structure and surface composition could be the use of irreversible adsorption of adatoms. Very recently, we have shown that this electrochemical methodology is an excellent tool to quantify the amount of (1 1 1) and (1 0 0) ordered domains on the surface of both bulk and Pt nanoparticle electrodes [35–38]. Nevertheless, unfortunately, this procedure has been only checked for the case of pure Pt surfaces and much more work would be necessary to apply this method to binary substrates.

The strong influence of Ir on the PtIr nanoparticles behaviour could also be explained by considering that the presence of Ir on the surface not only decreases the density of Pt(1 0 0) sites on the surface but also disrupts the long range order of the Pt(1 0 0) terraces that could be present on the surface of the Pt nanoparticles. As it has been pointed out in Refs. [7] and [8] with stepped surfaces vicinal to Pt(1 0 0), the bidimensional long range order has a great influence on its electrocatalytic behaviour. This double effect can justify the remarkable decrease of activity in comparison to that obtained for pure Pt.

From another point of view, the presence of Ir seems to cause a slight shift toward less positive potentials in the main oxidation

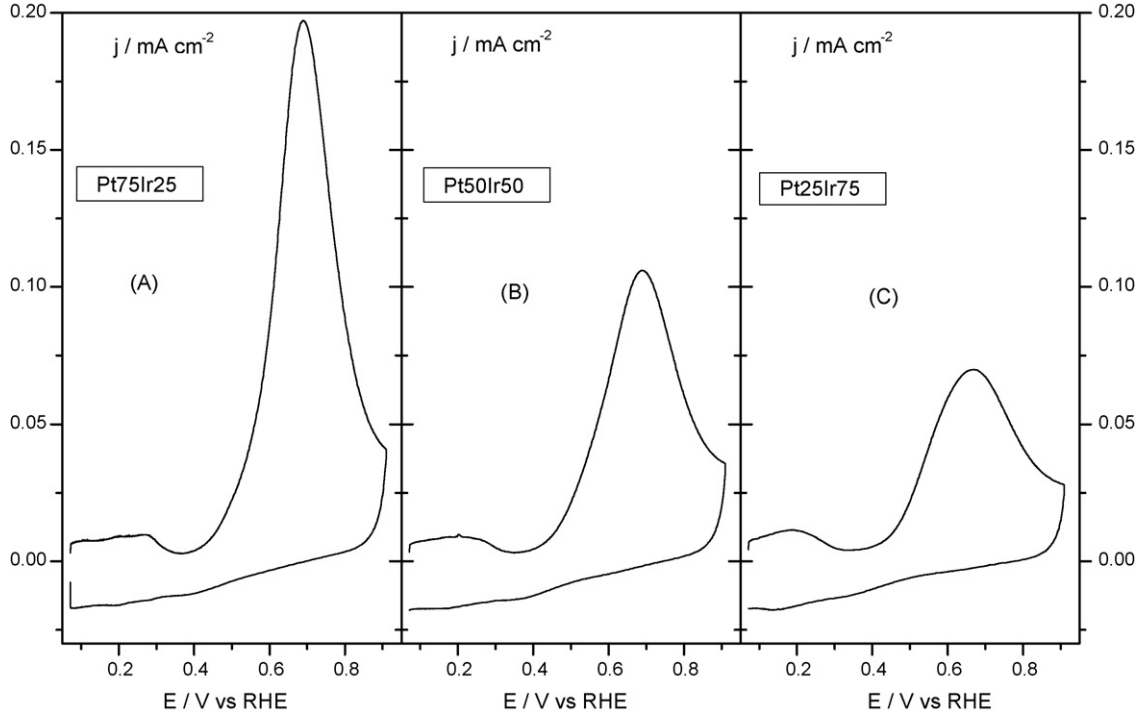

Fig. 4. Ammonia oxidation on $Pt_{75}Ir_{25}$ (A), $Pt_{50}Ir_{50}$ (B) and $Pt_{25}Ir_{75}$ (C) nanoparticles prepared in microemulsion. Test solution: NaOH 0.2 M + NH_3 0.1 M. Sweep rate: 10 mV s^{-1}.

peak. This shift is better shown at the highest amounts of Ir. Thus, with Ir nanoparticles, the peak potential is 60 mV lower than that obtained with Pt nanoparticles. It should be noted, however, that the difference decreases to only 15 mV for $Pt_{25}Ir_{75}$ whereas for $Pt_{75}Ir_{25}$ and $Pt_{50}Ir_{50}$ the main oxidation peak potential remains at the same value recorded when the electrode is made with pure Pt nanoparticles.

After analysing both peak current density and potential for ammonia oxidation on PtIr nanoparticles, it is necessary to pay attention to the onset potential of the oxidation process. Thus, although the oxidation peak potential for $Pt_{75}Ir_{25}$ and $Pt_{50}Ir_{50}$ alloys is very similar to that for Pt, the onset potential is less positive. Thus, the current density, in the low oxidation potential range, is higher for these PtIr binary nanoparticles than in the case of the pure Pt. As an example, at 0.55 V versus RHE, $Pt_{75}Ir_{25}$ shows a current density of 43.5 $\mu A\,cm^{-2}$, $Pt_{50}Ir_{50}$ of 40.9 $\mu A\,cm^{-2}$ and pure Pt of 18.7 $\mu A\,cm^{-2}$. This result is also in agreement with previous paper by de Vooys et al. [10] and Endo et al. [11,12], who have shown that the combination of Pt and Ir produces an enhancement for the ammonia oxidation, but only in the low oxidation potential region.

Once PtIr nanoparticles were analysed, other systems such as PtPd, PtRh and PtRu nanoparticles were screened. In the case of the pure metals, Pd, Rh and Ru showed no ammonia oxidation at all (Fig. 3). Similar results were also previously reported by de Vooys et al. [10]. These authors reported that on these metals ammonia is dehydrogenated at significantly lower potentials than on platinum or iridium, leading to the inert surface poison N_{ads} at much lower potentials than on platinum and iridium.

Some of the results obtained for these PtMe binary nanoparticles are reported in Fig. 5. The results indicate that, as in the case of Ir, the presence of Pd, Rh or Ru causes a decrease of the current density. Also, this decrease in current is higher than that could be expected assuming that the fraction of platinum in the surface that remains available toward ammonia oxidation has the same specific activity as that of pure Pt. For example, in the case of PtPd nanoparticles, the peak current density diminishes from 326 $\mu A\,cm^{-2}$ for pure platinum to only 103 $\mu A\,cm^{-2}$ for $Pt_{80}Pd_{20}$ nanoparticles. In the same way, for PtRh nanoparticles, the peak current density decreases to 150 $\mu A\,cm^{-2}$ for $Pt_{75}Rh_{25}$ nanoparticles. Thus, a decrease of 20 and 25% on the platinum amount causes the peak current density to diminish a 68% ($Pt_{80}Pd_{20}$) and a 54% ($Pt_{75}Rh_{25}$), respectively. However, as in the case of PtIr nanoparticles, the potential of the main peak and the onset potential shift toward less positive potential in both cases, being this shift much more important in the case of $Pt_{75}Rh_{25}$ nanoparticles. This suggests that the amount of the surface active sites has diminished, because the peak current decreased, but also the self-poisoning, a common characteristic observed in the oxidation of methanol and related compounds.

For PtRu nanoparticles, the results extracted from Fig. 5B reported how sensitive is the reaction to the presence of Ru. The oxidation of ammonia decreases very fast with the Ru content. Thus, for $Pt_{50}Ru_{50}$ a small current is observed whereas no oxidation is observed for $Pt_{20}Ru_{80}$ nanoparticles.

From the previous results, it appears that the use of these bimetallic nanoparticles does not significantly improve the activity obtained with pure platinum. Only in some of the samples containing Ir, Rh and Pd and for high Pt loadings, the onset potential shifts toward less positive potentials producing higher current densities than Pt. Therefore, at relatively low potentials, that would eventually correspond to suitable potential values for the anode in an ammonia fuel cell, some of the tested PtMe nanoparticles show higher current densities than those obtained for pure Pt nanoparticles.

Heretofore we have reported some of the results obtained for the ammonia oxidation using different PtMe nanoparticles, as well as the corresponding pure metal nanoparticles. As it was stated in Section 1, another interesting route to improve the reaction rate of structure sensitive reactions as it is the case of ammonia electrooxidation, it is to increase the density of the type of sites to which the reaction is sensitive. Therefore, and taking into account the high sensitivity of the ammonia electrooxidation to the presence of Pt(1 0 0) sites, some cubic Pt nanoparticles have been synthesised and studied for this probe reaction.

In previous contributions [39–41], it was shown that cubic Pt nanoparticles of ≈9 nm could be synthesised. The use of these cubic Pt nanoparticles showed a significant increase in the ammonia oxidation current density in relation to that found for polyoriented Pt nanoparticles [13,15]. However, the so-prepared cubic Pt nanoparticles were much larger in size than those pre-

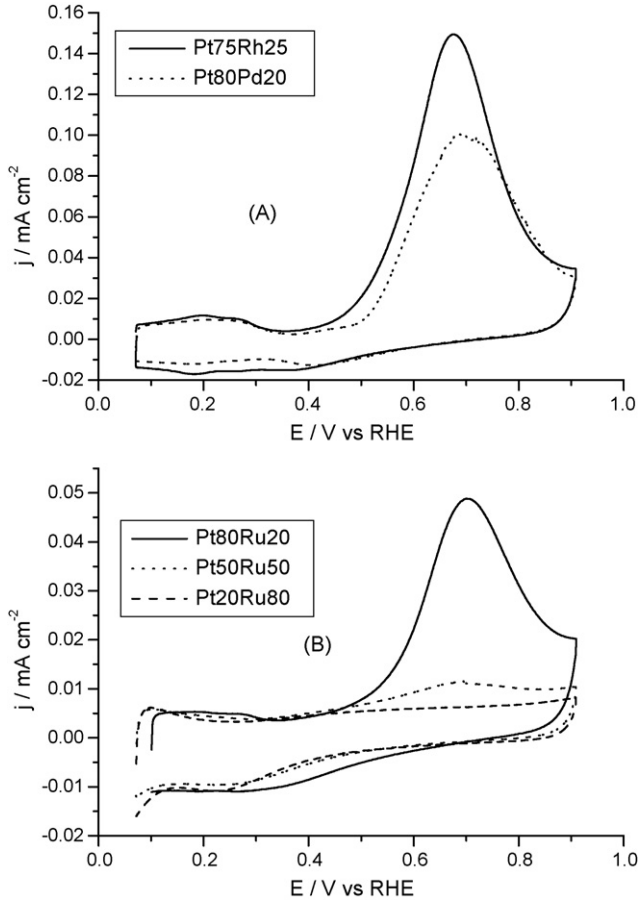

Fig. 5. Ammonia oxidation on $Pt_{75}Rh_{25}$ and $Pt_{80}Pd_{20}$ (A) and different PtRu nanoparticles (B) prepared in microemulsion. Test solution: NaOH 0.2 M + NH_3 0.1 M. Sweep rate: 10 mV s^{-1}.

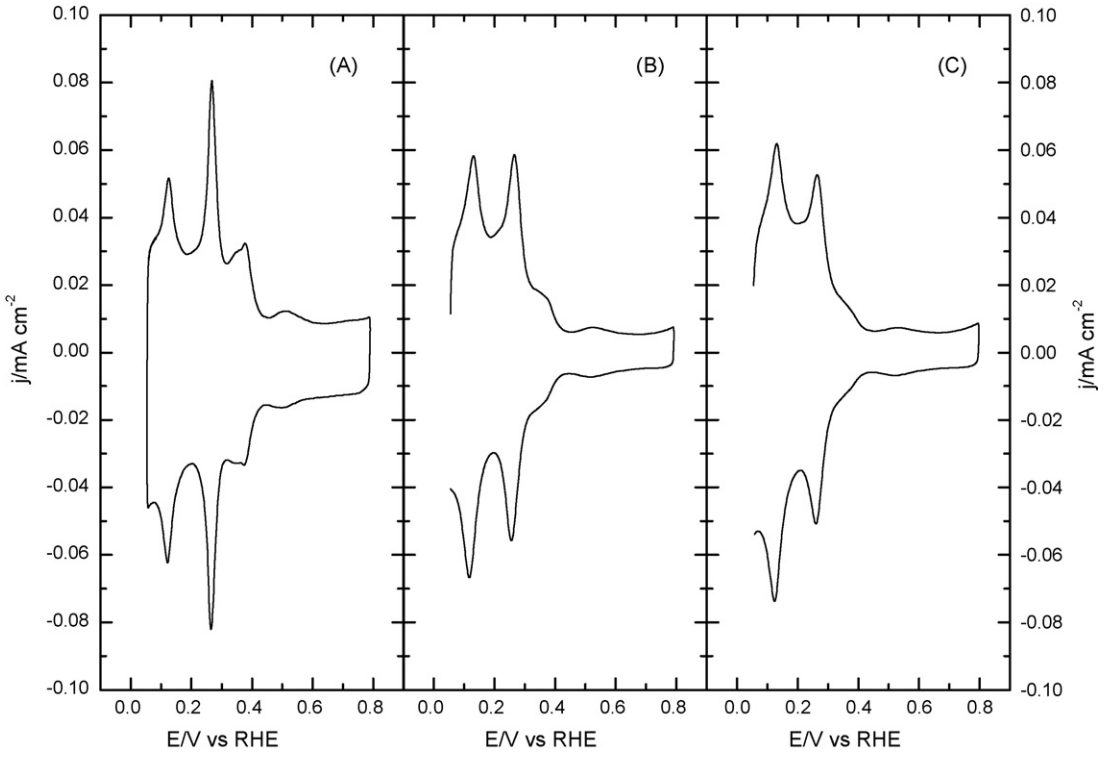

Fig. 6. Voltammograms corresponding to (A) 9-nm $Pt_{(1\,0\,0)}$, (B) 4-nm $Pt_{(1\,0\,0)}$ and (C) 4-nm $Pt_{(poly)}$ nanoparticles. Test solution: 0.5 M H_2SO_4, sweep rate 50 mV s^{-1}.

pared by the micellar method (≈3–4 nm). In this way, if the results obtained are normalised in relation to the current/mass of metal instead of to the current/area ratio of the metal, the effect of the surface structure became less relevant. Therefore, it appears interesting to synthesise preferential Pt(1 0 0) nanoparticles with a smaller size (around 4 nm) and compare its behaviour with the results found with Pt nanoparticles similar in size but without any preferential orientation. For this purpose, we have used the procedure described in Ref. [25] for the synthesis of small (≈4 nm) cubic Pt nanoparticles.

Fig. 6 shows the characteristic voltammetric profiles of the different Pt nanoparticles in 0.5 M sulphuric acid. The definition and the symmetry of the adsorption states are indicative of the surface cleanliness. For 9-nm cubic Pt nanoparticles (Fig. 6A) a very sharp peak at 0.27 V that corresponds to the border of (1 0 0) terraces and to (1 0 0) steps is observed. In addition, the well-marked state at 0.37 V, typical of (1 0 0) terrace sites, is clearly defined. These results point out that these Pt nanoparticles have a (1 0 0) preferential surface structure. Moreover, it is important to note that part of these Pt(1 0 0) sites correspond to relatively wide bidimensional (1 0 0) terraces, as suggested by the peak at 0.37 V. Fig. 6B and C show both voltammetric profiles very similar to that reported for polycrystalline platinum electrodes, although, in the case of the small cubic nanoparticles (Fig. 6B) a very clear shoulder around 0.35 V, characteristic of small (1 0 0) terraces, is observed.

Fig. 7 shows the ammonia oxidation voltammetric profiles corresponding to the three kinds of Pt nanoparticles (≈9 nm cubic Pt, ≈4 nm cubic Pt and ≈4 nm polyoriented Pt nanoparticles). The results obtained can easily be explained in terms of the amount of Pt(1 0 0) sites present at the surface of the nanoparticles. As it is expected the biggest nanoparticles show higher reactivity. However, especially interesting are the results found for the smallest Pt nanoparticles. Thus, 4-nm cubic Pt nanoparticles show a significantly higher current density than that obtained for nanoparticles of similar size but with a poly-oriented surface, indicating again the extremely high sensitivity if this reaction toward the presence of (1 0 0) Pt surface sites.

In summary, Fig. 8A compares the ammonia oxidation for the most promising PtMe nanoparticles to those corresponding to pure polyoriented Pt nanoparticles. As it was previously

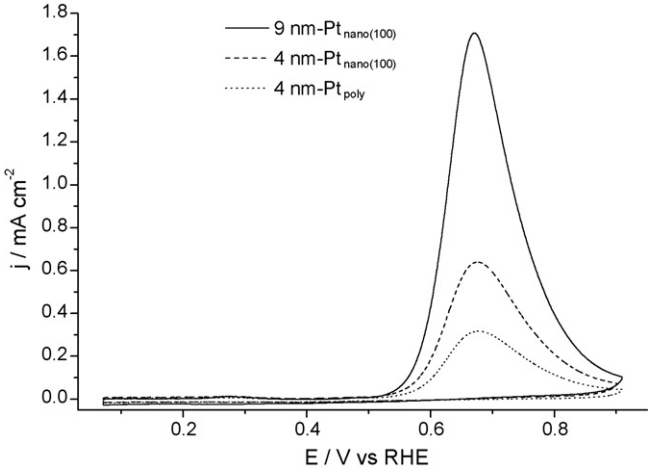

Fig. 7. Ammonia oxidation on different Pt nanoparticles. Test solution: NaOH 0.2 M + NH_3 0.1 M. Sweep rate: 10 mV s^{-1}.

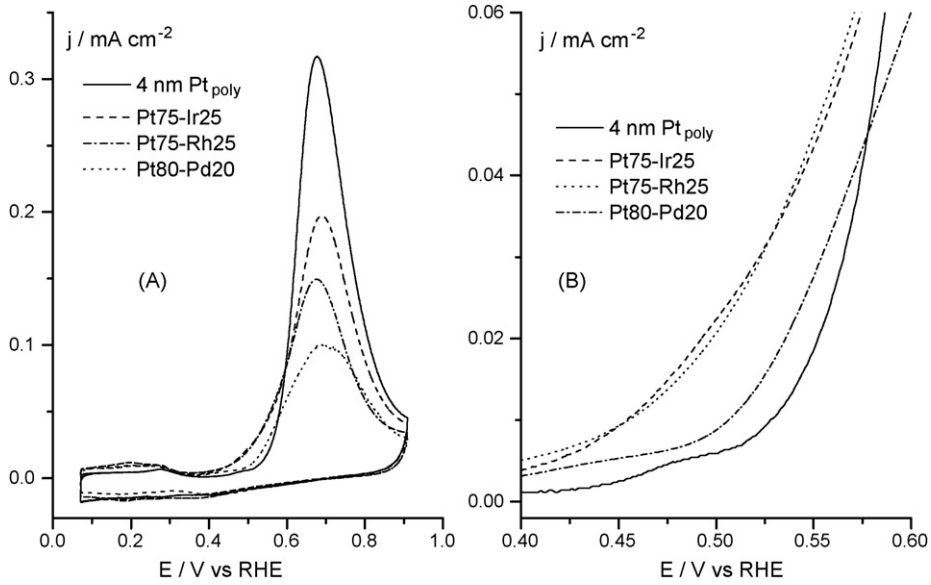

Fig. 8. Ammonia oxidation on different Pt and Pt–metal nanoparticles (A). (B) Zoomed image of the plot shown in (A). Test solution: NaOH 0.2 M + NH_3 0.1 M. Sweep rate: 10 mV s^{-1}.

commented, and in all binary nanoparticles, an important loss of maximum activity was observed after adding the second metal. In addition, the decrease in current is higher than that expected from atomic composition modification, pointing out not only the importance of the amount of Pt(1 0 0) surface sites but also its long range order. However, in the lower potential region (Fig. 8B) it is clear that $Pt_{75}Rh_{25}$ and $Pt_{75}Ir_{25}$ produce higher current densities than that observed for Pt nanoparticles.

Chronoamperometry measurements at 0.6 V were also performed to evaluate the electrocatalytic activity towards ammonia oxidation of some of the samples. As it can be appreciated in Fig. 9, ≈9 nm cubic Pt produces the highest current density after 1200 s (≈111 μA cm^{-2}). In addition, the current densities obtained for the rest of the nanoparticles correlate well with the results obtained in the voltammetric experiments (Fig. 8A). Thus, current density values of 28, 19, 17, 12 and 9 μA cm^{-2} for 4-nm cubic Pt, 4 nm polyoriented Pt, $Pt_{75}Ir_{25}$, $Pt_{80}Pd_{20}$ and $Pt_{75}Rh_{25}$ nanoparticles were respectively obtained.

Finally, it is important to note that from a practical point of view not only high currents are desirable but also long time stabilities of the electrocatalysts are expected. In this way, more work is still in progress in order to analyse the stability of the samples during long-time ammonia oxidation. These experiments will be carried out not only with some of the reported binary nanoparticles but also with the (1 0 0) preferentially oriented Pt nanoparticles.

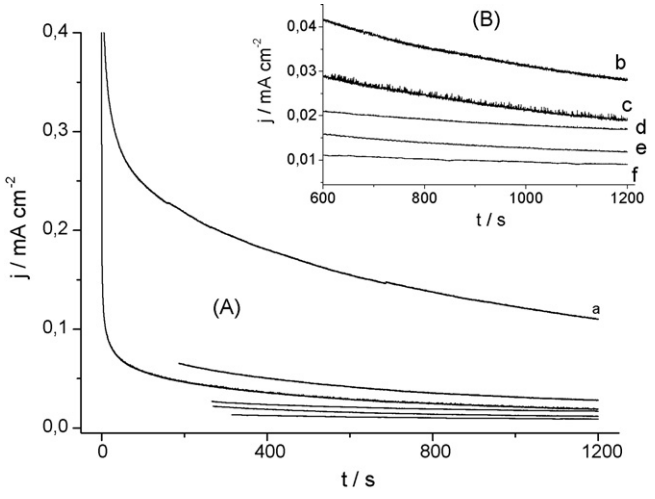

Fig. 9. Chronoamperometric measurements at 0.6 V for (a) 9-nm $Pt_{(1\,0\,0)}$, (b) 4-nm $Pt_{(1\,0\,0)}$, (c) 4-nm $Pt_{(poly)}$, (d) $Pt_{75}Ir_{25}$, (e) $Pt_{80}Pd_{20}$ and (f) $Pt_{75}Rh_{25}$ nanoparticles. (B) Zoomed image of the plot shown in (A). Test solution: NaOH 0.2 M + NH_3 0.1 M.

4. Conclusions

In this work, ammonia oxidation on different PtMe binary nanoparticles as well as on Pt nanoparticles of different surface structure is reported. For binary nanoparticles, Pt was chosen as base metal because the surface poison N_{ad} is formed at higher potentials when compared with the other metals. The choice of the second metal was based on its ability to dehydrogenate ammonia forming NH_x species and also as a possible inhibitor of the N_{ad}. In these conditions Pt would be able to oxidise the dehydrogenate species without significant poisoning, thus improving the electrocatalysis of the reaction. In this way, apart from Ir, which was found to show some activity for ammonia oxidation, Pd, Rh and Ru were chosen because of their previously reported dehydrogenation properties for ammonia, what made those pure metals inactive toward the ammonia electrooxidation.

As a general result, the incorporation of a second metal produces an important decrease on the ammonia oxidation current density. In addition, this decrease in the current density was higher than that expected from the modification on the atomic composition in the binary nanoparticles. This important drop on the current density seems also to be related to a decrease of the

density of (1 0 0) Pt surface sites as well as to the decrease of the dimensions of the small (1 0 0) domains of Pt on the surface of the nanoparticles that are particularly actives for ammonia oxidation. These results would be in agreement with the previously reported sensitivity of ammonia toward the density of the (1 0 0) Pt sites and the dimension of the (1 0 0) domains, on which exclusively this reaction takes place. Among all binary nanoparticles evaluated, only $Pt_{75}Ir_{25}$ and $Pt_{75}Rh_{25}$ nanoparticles show, at the low potential range, an enhancement of the oxidation density current with respect to the behaviour found for pure platinum.

Ammonia oxidations on Pt nanoparticles of different sizes and different surface structures/shapes have been also reported. Large (9 nm) and small (4 nm) Pt nanoparticles with a preferential (1 0 0) orientation, show an important increase of the ammonia oxidation current density in respect to that found for small (4 nm) Pt nanoparticles with a polyoriented orientation. The enhancement observed for the preferentially (1 0 0) oriented Pt nanoparticles can be easily explained by the fact that both density and dimension of the Pt(1 0 0) domains are higher in the preferentially oriented than in the polyoriented Pt nanoparticles. In this way, the importance of controlling the surface structure is again highlighted not only in the case of bulk electrodes, as it was shown with single crystals [42], but also, as in this case, for nanoparticles.

The good agreement of the reported results with those previously published confirms that the electrocatalytic behaviour of 4 nm nanoparticles fits perfectly with that obtained with the corresponding bulk alloys. In this way, either surface properties such as hydrogen/anion adsorption–desorption or electrocatalytic activity toward ammonia oxidation are perfectly comparable for bulk and dispersed materials. This situation points out that no special size effects appear at this stage.

Acknowledgment

This work has been financially supported by the Ministerio de Ciencia y Tecnologia of Spain through the project CTQ2006-04071.

References

[1] M. Zamanzadeh, P.R. Warburton, Patent App. 20050034985 (2005).
[2] D.Y. Wang, W.T. Symons, R.J. Farhat, C.A. Valdes, E.M. Briggs, K.K. Polikarpus, J. Kupe, Patent App. 20040118703 (2004).
[3] B.H. Timmer, K.M. van Delft, R.P. Otjes, W. Olthuis, A. van den Berg, Anal. Chim. Acta 507 (1) (2004) 137.
[4] M. Aslam, V.A. Chaudhary, I.S. Mulla, S.R. Sainkar, A.B. Mandale, A.A. Belhekar, K. Vijayamohanan, Sens. Actuat. A-Phys. 75 (2) (1999) 162.
[5] K. Kordesch, J. Gsellmann, M. Cifrain, S. Voss, V. Hacker, R.R. Aronson, C. Fabjan, T. Hejze, J. Daniel-Ivad, J. Power Sources 80 (1999) 190.
[6] F.J. Vidal-Iglesias, N. García-Aráez, V. Montiel, J.M. Feliu, A. Aldaz, Electrochem. Commun. 5 (2003) 22.
[7] F.J. Vidal-Iglesias, J. Solla-Gullón, V. Montiel, J.M. Feliu, A. Aldaz, J. Phys. Chem. B 109 (2005) 12914.
[8] V. Rosca, T.M. Koper, Phys. Chem., Chem. Phys. 8 (2006) 2513.
[9] H. Gerischer, A. Mauerer, J. Electroanal. Chem. 25 (1970) 421.
[10] A.C.A. de Vooys, M.T.M. Koper, R.A. van Santen, J.A.R. van Veen, J. Electroanal. Chem. 506 (2001) 127.
[11] K. Endo, Y. Katayama, T. Miura, Electrochim. Acta 49 (2004) 1635.
[12] K. Endo, K. Nakamura, Y. Katayama, T. Miura, Electrochim. Acta 49 (2004) 2503.
[13] F.J. Vidal-Iglesias, J. Solla-Gullón, P. Rodríguez, E. Herrero, V. Montiel, J.M. Feliu, A. Aldaz, Electrochem. Commun. 6 (2004) 1080.
[14] J. Solla-Gullón, F.J. Vidal-Iglesias, E. Herrero, J.M. Feliu, A. Aldaz, Electrochem. Commun. 8 (2006) 189.
[15] J. Solla-Gullón, F.J. Vidal-Iglesias, P. Rodríguez, E. Herrero, J.M. Feliu, J. Clavilier, A. Aldaz, J. Phys. Chem. B 108 (36) (2004) 13573.
[16] N.N. Markovic, V. Radmilovic, P.N. Ross Jr., in: A. Wieckowski, E. Savinova, C. Vayenas (Eds.), Catalysis & Electrocatalysis at Nanoparticle Surfaces, Marcel Dekker, New York, 2003, p. 311.
[17] J.B. Nagy, A. Claerbout, in: K.L. Mittal y, D.O. Shah (Eds.), Surfactants in Solution, vol. 11, Plenum Press, New York, 1991, p. 363.
[18] M. Boutonnet, J. Kizling, P. Stenius, G. Marie, Colloids Surf. 5 (1982) 209.
[19] M.A. López-Quintela, J. Rivas, J. Colloid. Interf. Sci. 158 (1993) 446.
[20] M.L. Wu, D.H. Chen, T.C. Hung, Langmuir 17 (2001) 3877.
[21] J. Solla-Gullón, V. Montiel, A. Aldaz, J. Clavilier, J. Electroanal. Chem. 491 (2000) 69.
[22] J. Solla Gullón. Ph.D. Thesis, University of Alicante, 2003.
[23] R. Touroude, P. Girard, G. Maire, J. Kizling, M. Boutonnet-Kizling, P. Stenius, Colloids Surf. 67 (1992) 9.
[24] J. Solla-Gullón, F.J. Vidal-Iglesias, V. Montiel, A. Aldaz, Electrochim. Acta 49 (2004) 5079.
[25] S.Y. Zhao, S.H. Chen, S.Y. Wang, D.G. Li, H.Y. Ma, Lagmuir 18 (2002) 3315.
[26] J. Solla-Gullón, V. Montiel, A. Aldaz, J. Clavilier, Electrochem. Commun. 4 (2002) 716.
[27] J. Solla-Gullón, V. Montiel, A. Aldaz, J. Clavilier, J. Electrochem. Soc. 150 (2) (2003) E104.
[28] J. Solla-Gullón, A. Rodes, V. Montiel, A. Aldaz, J. Clavilier, J. Electroanal. Chem. 554 (2003) 273.
[29] R. Woods, in: Allen J. Bard (Ed.), Electroanalytical Chemistry, vol. 9, Marcel Dekker, New York, 1976, p. 1.
[30] Z. Jusys, J. Kaiser, R.J. Behm, Phys. Chem. Chem. Phys. 3 (2001) 4650.
[31] M.J. Weaver, S.C. Chang, L.W.H. Leung, X. Jiang, M. Rubel, M. Szklarczyk, D. Zurawski, A. Wieckowski, J. Electroanal. Chem. 327 (1992) 247.
[32] L. Colmenares, Z. Jusys, R.J. Behm, Langmuir 22 (2006) 10437.
[33] Z. Jusys, J. Kaiser, R.J. Behm, Electrochim. Acta 47 (2002) 3693.
[34] H.H. Brogersma, M. Draxler, M. de Ridder, P. Bauer, Surf. Sci. Rep. 62 (8) (2007) 63.
[35] P. Rodríguez, E. Herrero, J. Solla-Gullón, F.J. Vidal-Iglesias, A. Aldaz, J.M. Feliu, Electrochim. Acta 50 (2005) 3111.
[36] P. Rodríguez, E. Herrero, J. Solla-Gullón, F.J. Vidal-Iglesias, A. Aldaz, J.M. Feliu, Electrochim. Acta 50 (2005) 4308.
[37] P. Rodríguez, J. Solla-Gullón, F.J. Vidal-Iglesias, E. Herrero, A. Aldaz, J.M. Feliu, Anal. Chem. 77 (2005) 5317.
[38] P. Rodríguez, E. Herrero, A. Aldaz, J.M. Feliu, Langmuir 22 (25) (2006) 10329.
[39] T.S. Ahmadi, Z.L. Wang, T.C. Green, A. Henglein, M.A. El-Sayed, Science 272 (1996) 1924.
[40] J.M. Petroski, Z.L. Wang, T.C. Green, M.A. El-Sayed, J. Phys. Chem. B 102 (1998) 3316.
[41] R. Narayanan, M.A. El-Sayed, J. Phys. Chem. B 108 (2004) 5726.
[42] J. Clavilier, in: A. Wieckowski (Ed.), Interfacial Electrochemistry, Theory, Experiments and Applications, Marcel Decker, New York, 1999, p. 231.